Kinesin Spindle Protein (KSP) Inhibitors with 2,3-Fused Indole Scaffolds

ARTICLE *in* JOURNAL OF MEDICINAL CHEMISTRY · JULY 2010

Impact Factor: 5.45 · DOI: 10.1021/jm100476d · Source: PubMed

5054 *J. Med. Chem.* **2010,** *53,* 5054–5058
DOI: 10.1021/jm100476d

Journal of Medicinal Chemistry
Brief Article

Kinesin Spindle Protein (KSP) Inhibitors with 2,3-Fused Indole Scaffolds

Shinya Oishi,*[,†] Toshiaki Watanabe,[†] Jun-ichi Sawada,[‡] Akira Asai,[‡] Hiroaki Ohno,[†] and Nobutaka Fujii*[,†]

[†]*Graduate School of Pharmaceutical Sciences, Kyoto University, Sakyo-ku, Kyoto 606-8501, Japan, and* [‡]*Graduate School of Pharmaceutical Sciences, University of Shizuoka, Suruga-ku, Shizuoka 422-8526, Japan*

Received April 19, 2010

Mitotic kinesin spindle protein (KSP) is involved in the assembly of the bipolar spindle during cell division. On the basis of a common 2,3-fused indole substructure within the complex frameworks of terpendole E and other KSP inhibitors, the carbazoles with a bulky alkyl group were identified as a novel KSP inhibitory scaffold. Additionally, among several naturally occurring cell growth inhibitors with 2,3-fused indole structures, β-carboline alkaloids, harman and harmine, showed moderate inhibition of KSP.

Introduction

Mitosis is a highly regulated process to separate the replicated sister chromatids into the daughter cells during cell division. Among a number of kinesin motor proteins with a catalytic motor domain driven by ATP hydrolysis, kinesin spindle protein (KSP,[a] also known as Eg5), a member of the kinesin-5 family, is associated with mitotic spindle assembly in the early stages of mitosis.[1] A bipolar homotetramer of KSP cross-links and moves antiparallel microtubules apart to prompt centrosome separation.[2] Impairment of KSP induces mitotic arrest in prometaphase without affecting microtubules, resulting in apoptotic cell death.[3] Accordingly, significant efforts have been made in developing KSP inhibitors as potential antitumor agents[4] since the identification of the first KSP inhibitor, monastrol.[5]

Terpendole E **1** is a fungal-derived KSP inhibitor,[6] which was originally identified as a minor isolate of the acyl-CoA:cholesterol acyltransferase (ACAT) inhibitor.[7] The core structure of **1** consists of indole and diterpene moieties. HR22C16 **2** is also a cell membrane-permeable KSP inhibitor with a tetrahydro-β-carboline structure that is observed in a number of natural products.[8] Furthermore, moderate in vitro KSP inhibitory activity of *N*-substituted carbazole **3** was recently reported.[9,10] Although these three compounds apparently include an exquisite complex framework with cyclic and/or acyclic accessory substituents, it was envisaged that a 2,3-fused indole **4** would be the common minimal scaffold for KSP inhibitory activity (Figure 1).[11,12]

Recently, we have accomplished the facile preparation of carbazole derivatives, which represent 2,3-fused indole derivatives. Of note, carbazoles were obtained via one-pot consecutive reactions including *N*-arylation of anilines and the oxidative biaryl coupling in the presence of a palladium catalyst (Scheme 1).[13] A combination of aryl triflates **5** and

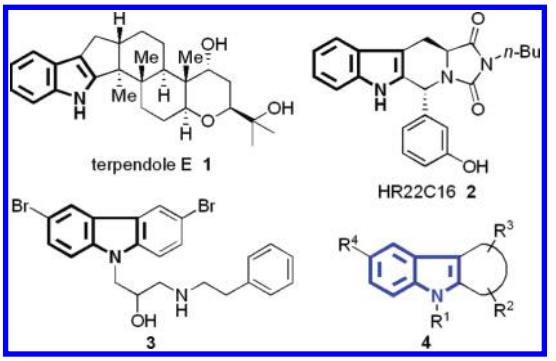

Figure 1. Structures of the reported KSP inhibitors **1**−**3** and the potential KSP inhibitory 2,3-fused indole scaffold **4**.

Scheme 1. One-Pot Synthesis of Carbazoles by *N*-Arylation and Oxidative Biaryl Coupling

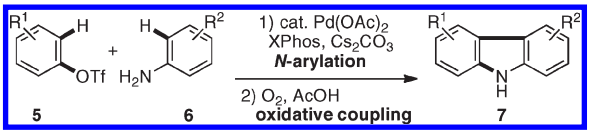

substituted anilines **6** can improve the structural diversity of carbazole derivatives **7**. By exploiting this carbazole library, the current study was undertaken to identify the minimal chemical space for KSP inhibitory activity from the precedent inhibitors. Furthermore, the structure−activity relationship study on carbazole-based KSP inhibitors and identification of KSP inhibitory alkaloids were also conducted.

Results and Discussion

Chemistry. A series of carbazole derivatives **8**−**10**, **11e**, and **12**−**15** were prepared by palladium-catalyzed one-pot *N*-arylation−oxidative biaryl coupling (Scheme 1),[13] except for the compounds indicated below. Carbazoles **12c**, **14b**, and **14f** were synthesized by palladium-catalyzed intramolecular C−H arylation of *N*-phenyl-2-haloaniline derivatives, which were obtained by *N*-arylation using *o*-chloroaniline

*To whom correspondence should be addressed. Phone: +81-75-753-4551. Fax: +81-75-753-4570. E-mail: soishi@pharm.kyoto-u.ac.jp (S.O.); nfujii@pharm.kyoto-u.ac.jp (N.F.).

[a] Abbreviations: ACAT, acyl-CoA:cholesterol acyltransferase; CENP-E, centromere-associated protein E; KSP, kinesin spindle protein; MKLP-1, mitotic kinesin-like protein 1.

 Published on Web 06/03/2010

16a/substituted bromobenzene **17a** or substituted anilines **16b**,**c**/*o*,*o*-dihalobenzenes **17b**,**c** (Scheme 2). Alternatively, arylation of an enamine intermediate prepared from 2-bromoaniline **16d** and cyclohexane-1,3-dione **18** conferred cyclohexenone-fused indole derivative **15c**. Carbazoles **12f**, **12j**, and **15a** were obtained by simple transformations such as *tert*-butyl modification of **12d**, saponification of **10f**, and *N*-methylation of **8f**, respectively. Several carbazoles or the related derivatives (**11a**,**f**, **12g**, **13b**, **14d**,**e**,**g**, **15b**,**e**,**f**) were prepared according to previous literature.[14]

Scheme 2. Synthesis of Carbazole Derivatives

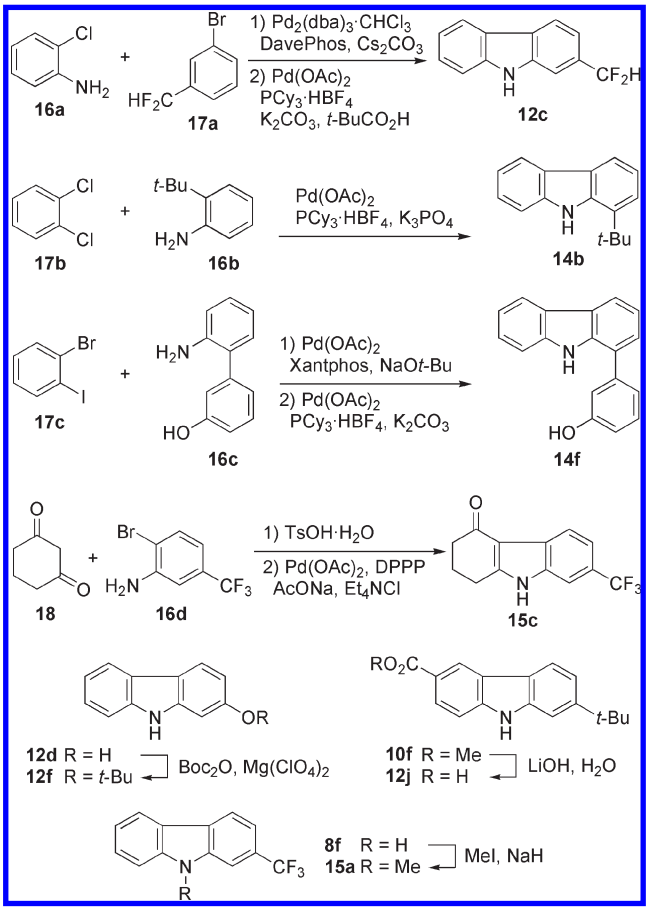

Identification of 2- or 3-Substituted Carbazoles and *β*-Carboline Alkaloids as KSP Inhibitors. A small library of substituted carbazoles **8**−**10**, which were prepared by one-pot carbazole synthesis, was screened using a microtubule-activated KSP ATPase assay. Among the 28 compounds examined, several carbazoles exhibited potent or moderate inhibition at 20 μM (Table 1). The most potent carbazoles **8e** (IC_{50} = 0.30 μM), **8f** (IC_{50} = 0.26 μM), and **9e** (IC_{50} = 0.95 μM) possess a bulky *t*-Bu or CF_3 groups at the carbazole 2- or 3-position. In contrast, these carbazoles did not inhibit the ATPase activity of the other motor proteins, centromere-associated protein E (CENP-E), kid, KIF-4, and mitotic kinesin-like protein 1 (MKLP-1) even at 20 μM, indicating the effects of the compounds are KSP-selective without direct binding to microtubules.

Inhibition of KSP activity by reported cell proliferation inhibitors[15] with a 2,3-fused indole substructure or related scaffolds was also investigated. Two topoisomerase II inhibitors, azatoxin **11a**[14d] and ellipticine **11b**,[15a] showed no inhibitory activity. Tryprostatin A **11c**,[15b] fumitremorgin C **11d**,[15b] murrayafoline A **11e**,[15c] and a substituted carbazole **11f**,[14g] which were reported to arrest the cell cycle in the G2/M-phase, did not inhibit the KSP motor activity (Figure 2). Interestingly, moderate inhibitory activity of KSP using *β*-carboline alkaloids, harman **11g** (IC_{50} = 32 μM) and harmine **11h** (IC_{50} = 38 μM), was observed. These compounds were previously reported to exhibit cytotoxicity, mutagenic, and neurotoxic effects by binding to DNA or through topoisomerase I/II inhibition.[16] This novel KSP inhibitory effect may be a secondary mode-of-action for the potent cytotoxicity of aromatic *β*-carboline alkaloids.

The bioactivities of the KSP inhibitory compounds **8e**,**f**, **9e**, and **11g**,**h** on topoisomerases I and II were examined (Figure 3) because the chemical space around the 2,3-fused indole derivatives appears to be shared among the known KSP and topoisomerase inhibitors. Harmine **11h** inhibited the DNA relaxation mediated by topoisomerases, whereas no inhibitory activities on either topoisomerases were observed when carbazoles **8e**,**f** and **9e** were present,[17]

Table 1. Structures and KSP Inhibitory Activities of the Substituted Carbazoles Screened

compound		R^1	R^2	% inhibition[a]
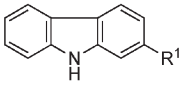	**8a**	H		10
	8b	Me		51
	8c	OMe		3
	8d	Ph		1
	8e	*t*-Bu		100
	8f	CF_3		100
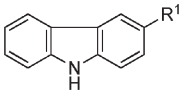	**9a**	F		28
	9b	Me		31
	9c	OMe		15
	9d	Ph		1
	9e	CF_3		93
	9f	CO_2Me		3
	9g	CO_2Bn		2
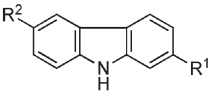	**10a**	Me	F	79
	10b	Me	CF_3	71
	10c	Me	CO_2Me	0
	10d	Me	COMe	94
	10e	OMe	CO_2Me	15
	10f	*t*-Bu	CO_2Me	69
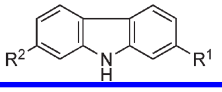	**10g**	Me	CO_2Me	2
	10h	Me	Ph	0

compound		R^1	R^2	% inhibition[a]
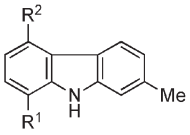	**10i**	CO_2Me	H	0
	10j	H	CO_2Me	39
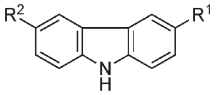	**10k**	Me	CF_3	69
	10l	Me	CO_2Me	1
	10m	*t*-Bu	CO_2Me	11
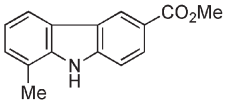	**10n**			1
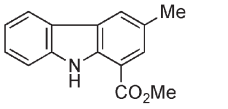	**10o**			0

[a] 20 μM of each carbazole was employed for the KSP ATPase assay.

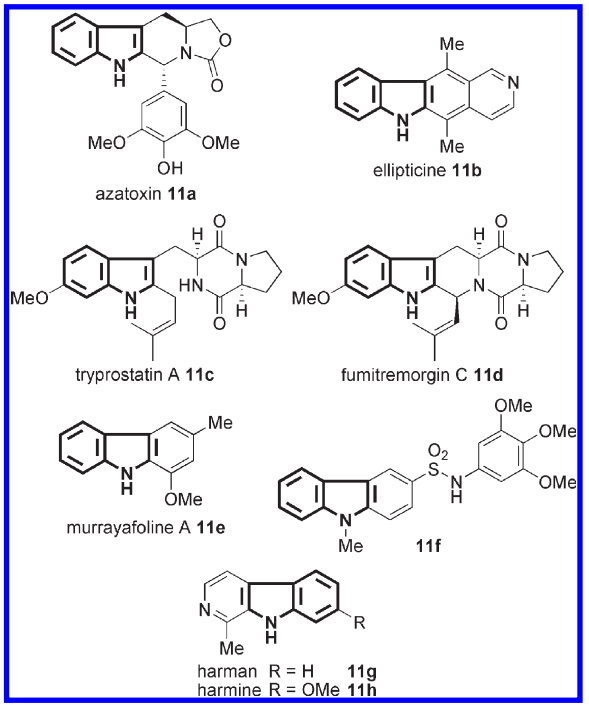

Figure 2. Structures of the natural products or the related compounds with a 2,3-fused indole substructure evaluated for KSP inhibitory activity.

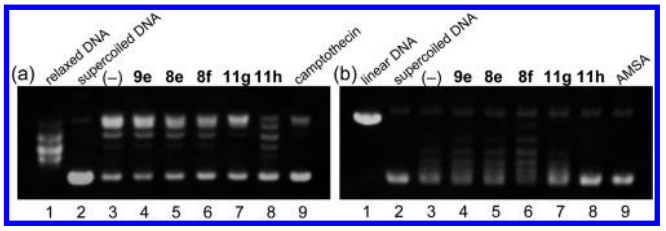

Figure 3. Effects of carbazoles **8e**,**f**, **9e**, and β-carbolines **11g**,**h** (100 μM) on DNA topoisomerases I [topo I, (a)] and II [topo II, (b)]. Lane 1: DNA marker; lane 2, supercoiled DNA; lane 3, DNA/enzyme; lane 4, DNA/enzyme+**9e**; lane 5, DNA/enzyme+**8e**; lane 6, DNA/enzyme+**8f**; lane 7, DNA/enzyme+**11g**; lane 8, DNA/enzyme+**11h**; lane 9, DNA/enzyme+camptothecin (for topo I) or +AMSA (for topo II).

supporting the notion that these carbazoles are specific KSP inhibitors.

Structure−Activity Relationship Study of Carbazole-Based Inhibitors. On the basis of the advantageous potency and selectivity for KSP inhibition by **8e**,**f** and **9e**, a further structure−activity relationship study was performed for carbazole derivatives (Table 2). KSP ATPase inhibition and antiproliferative effects were evaluated. Carbazoles **12a**,**b** and CF_2H-substituted **12c**, which include a smaller number of Me- and F-substituting groups on the benzyl position, exhibited less potent KSP inhibitory activity compared with carbazoles **8e** and **8f**, respectively. Insertion of an ether linkage between the carbazole core and the bulky alkyl group (**12e**,**f**) and modification with carbonyl groups (**12g**−**i**) were ineffective in improving the bioactivity. Moderate to potent KSP inhibitory activity of **10f** and **12k** with the secondary accessory 6-CO_2Me and 7-CF_3 groups, respectively, was observed, while no cell growth inhibition was exhibited at 60 μM. For the carbazole 3-position, modification with the *t*-Bu group provided the best inhibitor **13a** testified by in vitro KSP and cell proliferation assays. 1-Substituted carbazoles **14a**−**f** and 1-phenyl-β-carboline **14g**, which resemble the podophyllotoxin-like scaffold, showed no or less potent KSP inhibitory activity.

Investigation of additional modifications onto 2- or 3-substituted carbazole derivatives was also conducted (Table 3). *N*-Methylation of carbazole **8f** led to a significant decrease in the inhibitory activity [IC_{50} (**15a**) = 5.6 μM]. Cyclohexene- or cyclohexenone-fused derivatives **15b**,**c** failed to inhibit the KSP ATPase even at 20 μM. Carbazoles with an additional saturated or aromatic fused ring structure at 2,3- or 1,2-positions exhibited moderate KSP inhibitory activity. These results indicate that the planar tricyclic structure of carbazoles with a single bulky substituting group is the minimal scaffold for KSP inhibition and that *t*-Bu- and CF_3-groups at the 2- or 3-position are the most favorable accessory groups.

These carbazoles **8e**,**f**, **9e**, and **13a** exhibited up to 30-fold more potency in KSP ATPase inhibition compared with the known KSP inhibitor **2**, while similarly or less potent inhibition against HeLa cell growth was observed. The low cell membrane permeability or unspecific binding to the secondary biomolecules could be attributable to the incompatible results.

Table 2. Structure−Activity Relationships of Carbazoles That Inhibit KSP

compound		R^1	R^2	KSP ATPase IC_{50} (μM)[a,b]	cell growth IC_{50} (μM)[a,c]
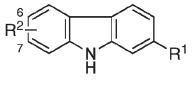	**8b**	Me	H	22	-[e]
	8e	*t*-Bu	H	0.30	40
	8f	CF_3	H	0.26	11
	12a	Et	H	2.8	-[e]
	12b	*i*-Pr	H	1.5	19
	12c	CF_2H	H	0.87	46
	12d	OH	H	-[d]	-[e]
	12e	OCF_3	H	0.51	29
	12f	O*t*-Bu	H	3.2	-[e]
	12g	CO_2H	H	-[d]	-[f]
	12h	CO_2Me	H	11	-[e]
	12i	CHO	H	13	-[e]
	10f	*t*-Bu	6-CO_2Me	0.39	-[e]
	12j	*t*-Bu	6-CO_2H	11	-[e]
	12k	*t*-Bu	7-CF_3	1.4	-[e]
	10a	Me	6-F	7.5	-[e]
	10d	Me	6-COMe	1.6	51
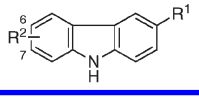	**9e**	CF_3	H	0.95	14
	13a	*t*-Bu	H	0.24	6.5
	13b	CHO	H	17	-[e]
	10b	CF_3	7-Me	11	35
	10k	CF_3	6-Me	8.8	-[e]

compound		R	X	KSP ATPase IC_{50} (μM)[a,b]	cell growth IC_{50} (μM)[a,c]
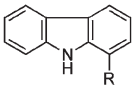	**14a**	Me	-	23	-[e]
	14b	*t*-Bu	-	14	41
	14c	CF_3	-	3.3	-[e]
	14d	CH_2OH	-	-[d]	-[f]
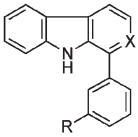	**14e**	H	CH	-[d]	-[f]
	14f	OH	CH	-[d]	-[f]
	14g	OH	N	-[d]	-[f]
	2 (HR22C16)			7.1	8.6

[a] IC_{50} values were derived from the dose−response curves generated from triplicate data points. [b] Inhibition of microtubule-activated KSP ATPase activity. [c] Cytotoxic activity against HeLa cells after 48-h exposure to the compound. [d] Less than 50% inhibition at 20 μM. [e] Less than 50% inhibition at 60 μM. [f] Not tested.

Table 3. Structure−Activity Relationships of Carbazoles and the Related Compounds for Inhibition of KSP

compound		KSP ATPase IC_{50} (μM)[a,b]	cell growth IC_{50} (μM)[a,c]
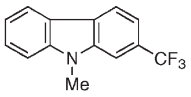	**15a**	5.6	-[e]
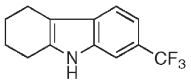	**15b**	-[d]	-[f]
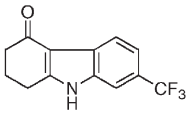	**15c**	-[d]	-[f]
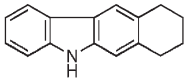	**15d**	25	-[e]
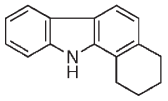	**15e**	1.6	30
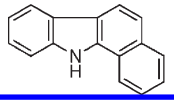	**15f**	4.6	-[e]

[a] IC_{50} values were derived from the dose−response curves generated from triplicate data points. [b] Inhibition of microtubule-activated KSP ATPase activity. [c] Cytotoxic activity against HeLa cells after 48 h exposure to the compound. [d] Less than 50% inhibition at 20 μM. [e] Less than 50% inhibition at 60 μM. [f] Not tested.

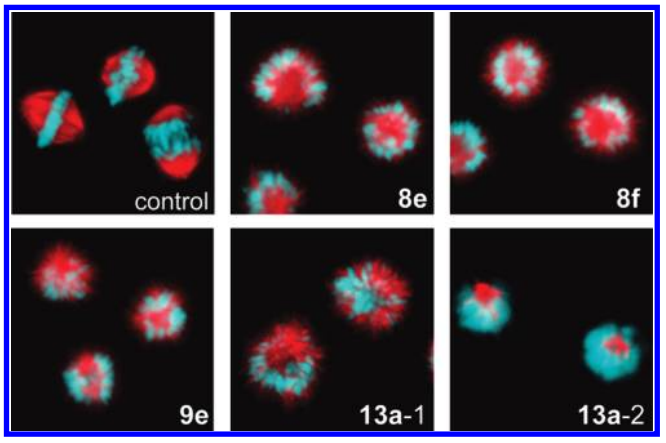

Figure 4. Monopolar spindle formation by treatment of HeLa cells with carbazole derivatives (**8e,f**, **9e**: 80 μM; **13a**: 16 μM). Chromosomes are colored in blue, and α-tubulin in red.

However, high rates of HeLa cells were arrested in the M-phase after 20 h exposure to 32 μM of the compounds [relative mitotic index (% induction of 0.1 μM taxol): **8e**, 37%; **8f**, 70%; **9e**, 57%; **13a**, 76%]. The arrested cells in the presence of the carbazoles **8e**,**f**, **9e**, and **13a** had monopolar spindles, the typical phenotype of KSP suppression, as a major phenotype (Figure 4). It is of note that another phenotype of cell cycle arrest at the G2/M-phase with incomplete chromosome condensation was also observed as a quite minor population following treatment with carbazole **13a** (Figure 4: **13a**-2).[18]

Conclusions

We have identified a novel inhibitory carbazole scaffold against mitotic kinesin KSP by comparative classification of the complex structures in KSP specific inhibitors and by using a library of carbazole derivatives prepared by the one-pot carbazole synthesis. In addition, among several naturally occurring cell growth inhibitors with 2,3-fused indole structures, moderate KSP inhibition of two β-carboline alkaloids, harman and harmine, was demonstrated. An additional structure−activity relationship study accentuated that carbazoles with a bulky alkyl group at the 2- or 3-position are the key substructures relevant to the potent and selective KSP inhibitory scaffold. Many natural secondary metabolites often have complicated structures and bind to multiple target molecules with moderate potency. This approach can also be used to identify the lead scaffold within natural products for further optimization processes, as well as to reveal the undefined mode of action of natural products.

Experimental Section

General Procedure for the Synthesis of Carbazoles. Toluene (0.4 mL) was added to a flask containing aryl triflate **5** (0.20 mmol), aniline **6** (0.22 mmol), $Pd(OAc)_2$ (10 mol %), XPhos (15 mol %), and Cs_2CO_3 (0.24 mmol) under an argon atmosphere. The mixture was stirred at 100 °C for 1−2 h and then stirred at room temperature for 5 min. AcOH (1.6 mL) was added to the mixture, and an oxygen balloon was connected to the reaction vessel. The reaction mixture was stirred at 100 or 120 °C for 7−20 h. After cooling, the reaction mixture was diluted with ethyl acetate, washed with saturated $NaHCO_3$, dried over $MgSO_4$, and concentrated in vacuo. Crude material was purified by flash chromatography to afford the desired carbazole. The purity of the compounds was determined as >95% by HPLC analysis or combustion analysis. The characterization data of newly synthesized carbazoles are shown in the Supporting Information.

KSP ATPase Assay. The microtubules-stimulated KSP ATPase reaction was performed in a reaction buffer [20 mM PIPES-KOH (pH 6.8), 25 mM KCl, 2 mM $MgCl_2$, 1 mM EGTA-KOH (pH 8.0)] containing 38 nM of the KSP motor domain and 350 nM microtubules in 96-well half area plates (Corning). Each chemical in DMSO at different concentrations was diluted 12.5-fold with the chemical dilution buffer [10 mM Tris-OAc (pH7.4), 0.04% (v/v) NP-40]. After preincubation of 9.7 μL of the enzyme solution with 3.8 μL of each chemical solution at 25 °C for 30 min, the ATPase reaction was initiated by the addition of 1.5 μL of 0.3 mM ATP and followed by incubation at 25 °C for a further 15 min. The reaction was terminated by the addition of 15 μL of the Kinase-Glo Plus reagent (Promega). The ATP consumption in each reaction was measured as the luciferase-derived luminescence by ARVO Light (PerkinElmer). At least three experiments were performed per condition, and the averages and standard deviations of inhibition rates in each condition were evaluated.

Growth Inhibition Assay. HeLa cells were cultured in DMEM medium (Wako) supplemented with 10% (v/v) FCS and antibiotics at 37 °C in a 5% CO_2 incubator. Growth inhibition assays using HeLa cells were performed in 96-well plates (Greiner). HeLa cells were seeded at 5000 cells/well in 50 μL of DMEM and placed for 6 h. Chemicals in DMSO were diluted 100-fold with the culture medium in advance. Following the addition of 40 μL of the fresh culture medium, 30 μL of the chemical diluents were also added to the cell cultures. The final volume of DMSO in the medium was equal to 0.25% (v/v). The cells under chemical treatment were incubated for a further 72 h. The wells in the plates were washed twice with DMEM medium (phenol-red minus) supplemented with 5% (v/v) FCS and antibiotics. After 1 h incubation with 100 μL of the medium, the cell culture in each well was supplemented with 20 μL of the MTS reagent (Promega), followed by incubation for an additional 40 min. Absorbance at 590 nm of each well was measured using a VersaMax plate reader (Molecular Devices).

Acknowledgment. This research was supported in part by the Targeted Protein Research Program and Grants-in-Aid for Scientific Research from the Ministry of Education, Culture, Sports, Science and Technology, Japan. We are indebted to Tomoko Kurose for excellent technical assistance. T.W. is grateful for the JSPS Research Fellowships for Young Scientists.

Supporting Information Available: Experimental procedures, characterization, and bioassay data. This material is available free of charge via the Internet at http://pubs.acs.org.

References

(1) Sawin, K. E.; LeGuellec, K.; Philippe, M.; Mitchison, T. J. Mitotic spindle organization by a plus-end-directed microtubule motor. *Nature* **1992**, *359*, 540–543.

(2) Kapitein, L. C.; Peterman, E. J.; Kwok, B. H.; Kim, J. H.; Kapoor, T. M.; Schmidt, C. F. The bipolar mitotic kinesin Eg5 moves on both microtubules that it crosslinks. *Nature* **2005**, *435*, 114–118.

(3) (a) Tao, W.; South, V. J.; Zhang, Y.; Davide, J. P.; Farrell, L.; Kohl, N. E.; Sepp-Lorenzino, L.; Lobell, R. B. Induction of apoptosis by an inhibitor of the mitotic kinesin KSP requires both activation of the spindle assembly checkpoint and mitotic slippage. *Cancer Cell* **2005**, *8*, 49–59. (b) Marcus, A. I.; Peters, U.; Thomas, S. L.; Garrett, S.; Zelnak, A.; Kapoor, T. M.; Giannakakou, P. Mitotic kinesin inhibitors induce mitotic arrest and cell death in Taxol-resistant and -sensitive cancer cells. *J. Biol. Chem.* **2005**, *280*, 11569–11577.

(4) For recent reviews, see: (a) Sarli, V.; Giannis, A. Inhibitors of mitotic kinesins: next-generation antimitotics. *ChemMedChem* **2006**, *1*, 293–298. (b) Jackson, J. R.; Patrick, D. R.; Dar, M. M.; Huang, P. S. Targeted anti-mitotic therapies: can we improve on tubulin agents? *Nat. Rev. Cancer* **2007**, *7*, 107–117. (c) Matsuno, K.; Sawada, J.; Asai, A. Therapeutic potential of mitotic kinesin inhibitors in cancer. *Expert Opin. Ther. Patents* **2008**, *18*, 253–274. (d) Sarli, V.; Giannis, A. Targeting the kinesin spindle protein: basic principles and clinical implications. *Clin. Cancer Res.* **2008**, *14*, 7583–7587.

(5) Mayer, T. U.; Kapoor, T. M.; Haggarty, S. J; King, R. W.; Schreiber, S. L.; Mitchison, T. J. Small molecule inhibitor of mitotic spindle bipolarity identified in a phenotype-based screen. *Science* **1999**, *286*, 971–974.

(6) Nakazawa, J.; Yajima, J.; Usui, T.; Ueki, M.; Takatsuki, A.; Imoto, M.; Toyoshima, Y. Y.; Osada, H. A novel action of terpendole E on the motor activity of mitotic Kinesin Eg5. *Chem. Biol.* **2003**, *10*, 131–137.

(7) (a) Huang, X. H.; Tomoda, H.; Nishida, H.; Masuma, R.; Omura, S. Terpendoles, novel ACAT inhibitors produced by *Albophoma yamanashiensis*. I. Production, isolation and biological properties. *J. Antibiot.* **1995**, *48*, 1–4. (b) X. Huang, H.; Nishida, H.; Tomoda, H.; Tabata, N.; Shiomi, K.; Yang, D. J.; Takayanagi, H.; Omura, S. Terpendoles, novel ACAT inhibitors produced by Albophoma yamanashiensis. II. Structure elucidation of terpendoles A, B, C and D. *J. Antibiot.* **1995**, *48*, 5–11.

(8) Hotha, S.; Yarrow, J. C.; Yang, J. G.; Garrett, S.; Renduchintala, K. V.; Mayer, T. U.; Kapoor, T. M. HR22C16: a potent small-molecule probe for the dynamics of cell division. *Angew. Chem., Int. Ed.* **2003**, *42*, 2379–2382.

(9) Okumura, H.; Nakazawa, J.; Tsuganezawa, K.; Usui, T.; Osada, H.; Matsumoto, T.; Tanaka, A.; Yokoyama, S. Phenothiazine and carbazole-related compounds inhibit mitotic kinesin Eg5 and trigger apoptosis in transformed culture cells. *Toxicol. Lett.* **2006**, *166*, 44–52.

(10) For patent information including the related carbazole compounds, see: Dhanak, D.; Knight, S. D.; Moore, M. L.; Newlander, K. A. PCT Int. Appl. WO2006005063, 2006.

(11) Similar scaffold identification approaches for other target molecules have been reported, see: (a) Koch, M. A.; Schuffenhauer, A.; Scheck, M.; Wetzel, S.; Casaulta, M.; Odermatt, A.; Ertl, P.; Waldmann, H. Charting biologically relevant chemical space: a structural classification of natural products (SCONP). *Proc. Natl. Acad. Sci. U.S.A.* **2005**, *102*, 17272–17277. (b) Nören-Müller, A.; Reis-Corrêa, I., Jr.; Prinz, H.; Rosenbaum, C.; Saxena, K.; Schwalbe, H. J.; Vestweber, D.; Cagna, G.; Schunk, S.; Schwarz, O.; Schiewe, H.; Waldmann, H. Discovery of protein phosphatase inhibitor classes by biology-oriented synthesis. *Proc. Natl. Acad. Sci. U.S.A.* **2006**, *103*, 10606–10611. (c) Reis-Corrêa, I., Jr.; Nören-Müller, A.; Ambrosi, H. D.; Jakupovic, S.; Saxena, K.; Schwalbe, H.; Kaiser, M.; Waldmann, H. Identification of inhibitors for mycobacterial protein tyrosine phosphatase B (MptpB) by biology-oriented synthesis (BIOS). *Chem. Asian J.* **2007**, *2*, 1109–1126. (d) Nören-Müller, A.; Wilk, W.; Saxena, K.; Schwalbe, H.; Kaiser, M.; Waldmann, H. Discovery of a new class of inhibitors of Mycobacterium tuberculosis protein tyrosine phosphatase B by biology-oriented synthesis. *Angew. Chem., Int. Ed.* **2008**, *47*, 5973–5977.

(12) Alternative nonindole based KSP inhibitors have been reported, for example: (a) Brier, S.; Lemaire, D.; Debonis, S.; Forest, E.; Kozielski, F. Identification of the protein binding region of *S*-trityl-L-cysteine, a new potent inhibitor of the mitotic kinesin Eg5. *Biochemistry* **2004**, *43*, 13072–13082. (b) Gartner, M.; Sunder-Plassmann, N.; Seiler, J.; Utz, M.; Vernos, I.; Surrey, T.; Giannis, A. Development and biological evaluation of potent and specific inhibitors of mitotic Kinesin Eg5. *ChemBioChem* **2005**, *6*, 1173–1177.

(13) (a) Watanabe, T.; Ueda, S.; Inuki, S.; Oishi, S.; Fujii, N.; Ohno, H. One-pot synthesis of carbazoles by palladium-catalyzed *N*-arylation and oxidative coupling. *Chem. Commun.* **2007**, 4516–4518. (b) Watanabe, T.; Oishi, S.; Fujii, N.; Ohno, H. Palladium-catalyzed direct synthesis of carbazoles via one-pot *N*-arylation and oxidative biaryl coupling: synthesis and mechanistic study. *J. Org. Chem.* **2009**, *74*, 4720–4726.

(14) (a) Forbes, E. J.; Stacey, M.; Tatlow, J. C.; Wragg, R. T. The synthesis of 1-, 2- and 3-trifluoromethylcarbazoles by the Fischer-indole method. *Tetrahedron* **1960**, *8*, 67–72. (b) Ohta, T.; Miyake, S.; Shudo, K. A trifluoromethanesulfonic acid-catalyzed reaction of arylhydrazines with benzene. *Tetrahedron Lett.* **1985**, *26*, 5811–5814. (c) Jash, S. S.; Biswas, G. K.; Bhattacharyya, S. K.; Bhattacharyya, P.; Chakraborty, A.; Chowdhury, B. K. Carbazole alkaloids from Glycosmis pentaphylla. *Phytochemistry* **1992**, *31*, 2503–2505. (d) Leteurtre, F.; Madalengoitia, J.; Orr, A.; Guzi, T. J.; Lehnert, E.; Macdonald, T.; Pommier, Y. Rational design and molecular effects of a new topoisomerase II inhibitor, azatoxin. *Cancer Res.* **1992**, *52*, 4478–4483. (e) Molina, P.; Fresneda, P. M.; Almendros, P. Fused carbazoles by tandem Aza Wittig/electrocyclic ring closure. Preparation of 6*H*-pyrido[4,3-*b*]-carbazole, 11*H*-pyrido[4,3-*a*]carbazole and 11*H*-pyrido[3,4-*a*]carbazole derivatives. *Tetrahedron* **1993**, *49*, 1223–1236. (f) Fabien, D.; Gilbert, K. Efficient synthesis of 1,2,3,4-tetrahydro-11*H*-benzo[*a*]carbazole and its regioselective oxidation. *Synlett* **2006**, *7*, 1021–1022. (g) Hu, L.; Li, Z. R.; Li, Y.; Qu, J.; Ling, Y. H.; Jiang, J. D.; Boykin, D. W. Synthesis and structure−activity relationships of carbazole sulfonamides as a novel class of antimitotic agents against solid tumors. *J. Med. Chem.* **2006**, *49*, 6273–6282. (h) Sanz, R.; Escribano, J.; Pedrosa, M. R.; Aguado, R.; Arnaiz, F. J. Dioxomolybdenum(VI)-catalyzed reductive cyclization of nitroaromatics: synthesis of carbazoles and indoles. *Adv. Synth. Catal.* **2007**, *349*, 713–718. (i) Hadjaz, F.; Yous, S.; Lebegue, N.; Berthelot, P.; Carato, P. A mild and efficient route to 2-benzyl tryptamine derivatives via ring-opening of β-carbolines. *Tetrahedron* **2008**, *64*, 10004–10008.

(15) (a) Goodwin, S.; Smith, A. F.; Horning, E. C. Alkaloids of *Ochrosia elliptica* Labill. *J. Am. Chem. Soc.* **1959**, *81*, 1903–1908. (b) Cui, C. B.; Kakeya, H.; Okada, G.; Onose, R.; Osada, H. Novel mammalian cell cycle inhibitors, tryprostatins A, B and other diketopiperazines produced by Aspergillus fumigatus. I. Taxonomy, fermentation, isolation and biological properties. *J. Antibiot.* **1996**, *49*, 527–533. (c) Cui, C. B.; Yan, S. Y.; Cai, B.; Yao, X. S. Carbazole alkaloids as new cell cycle inhibitor and apoptosis inducers from Clausena dunniana Levl. *J. Asian Nat. Prod. Res.* **2002**, *4*, 233–241.

(16) (a) Funayama, Y.; Nishio, K.; Wakabayashi, K.; Nagao, M.; Shimoi, K.; Ohira, T.; Hasegawa, S.; Saijo, N. Effects of β- and γ-carboline derivatives of DNA topoisomerase activities. *Mutat. Res.* **1996**, *349*, 183–191. (b) Cao, R.; Peng, W.; Chen, H.; Ma, Y.; Liu, X.; Hou, X.; Guan, H.; Xu, A. DNA binding properties of 9-substituted harmine derivatives. *Biochem. Biophys. Res. Commun.* **2005**, *338*, 1557–1563.

(17) Carbazoles **8e**,**f** and **9e** apparently activated the topoisomerase II-mediated relaxation. This activity was not due to the direct DNA relaxation by the compounds (see the Supporting Information).

(18) The reason of the unprecedented phenotype observed remains unsolved.